nature neuroscience

Chronic monoacylglycerol lipase blockade causes functional antagonism of the endocannabinoid system

Joel E Schlosburg[1,5], Jacqueline L Blankman[2,5], Jonathan Z Long[2], Daniel K Nomura[2], Bin Pan[3], Steven G Kinsey[1], Peter T Nguyen[1], Divya Ramesh[1], Lamont Booker[1], James J Burston[1], Elizabeth A Thomas[4], Dana E Selley[1], Laura J Sim-Selley[1], Qing-song Liu[3], Aron H Lichtman[1] & Benjamin F Cravatt[2]

Prolonged exposure to drugs of abuse, such as cannabinoids and opioids, leads to pharmacological tolerance and receptor desensitization in the nervous system. We found that a similar form of functional antagonism was produced by sustained inactivation of monoacylglycerol lipase (MAGL), the principal degradative enzyme for the endocannabinoid 2-arachidonoylglycerol. After repeated administration, the MAGL inhibitor JZL184 lost its analgesic activity and produced cross-tolerance to cannabinoid receptor (CB_1) agonists in mice, effects that were phenocopied by genetic disruption of *Mgll* (encoding MAGL). Chronic MAGL blockade also caused physical dependence, impaired endocannabinoid-dependent synaptic plasticity and desensitized brain CB_1 receptors. These data contrast with blockade of fatty acid amide hydrolase, an enzyme that degrades the other major endocannabinoid anandamide, which produced sustained analgesia without impairing CB_1 receptors. Thus, individual endocannabinoids generate distinct analgesic profiles that are either sustained or transitory and associated with agonism and functional antagonism of the brain cannabinoid system, respectively.

The endogenous cannabinoid (endocannabinoid) system[1] consists of two G protein–coupled receptors, CB_1 and CB_2, and their natural lipid ligands, *N*-arachidonoylethanolamine (anandamide)[2] and 2-arachidonoyglycerol (2-AG)[3,4]. The CB_1 receptor is highly expressed throughout the nervous system, where it mediates most of the neurobehavioral effects of cannabinoid agonists, such as Δ9-tetrahydrocannabinol (THC), the primary psychoactive component of marijuana[5]. The CB_2 receptor is only sparsely expressed in the brain and is instead found mainly on immune cells[5]. Unlike most other neurotransmitters, which are water soluble and stored in membrane-delineated vesicles before release, the endocannabinoids anandamide and 2-AG are hydrophobic neutral lipids that appear to be biosynthesized and released at the moment of their intended action (on-demand production[6]). These features indicate that the enzymes involved in endocannabinoid production and degradation are important regulators of signaling[7–9]. For instance, genetic[10,11] or pharmacological[12–15] disruption of fatty acid amide hydrolase (FAAH), the principal degradative enzyme for anandamide[16], elevates brain levels of anandamide and produces CB_1-dependent analgesia in multiple pain assays. A similar outcome is observed following acute blockade of the 2-AG–degrading enzyme MAGL, which raises 2-AG levels in the nervous system and reduces pain behavior[17,18]. Inhibition of MAGL, however, causes additional behavioral effects that are not observed following FAAH blockade, including hypomotility and hyperreflexia[17,19], which suggest that the enzyme has a broader effect on the brain cannabinoid system. In further support of this premise, MAGL inhibitors, but not FAAH inhibitors, augment depolarization-induced suppression of inhibition (DSI)[20] and excitation (DSE)[20,21], forms of synaptic plasticity that have been shown to require the CB_1 receptor[22] and the 2-AG biosynthetic enzyme diacylglycerol lipase-α[23,24].

The overlapping, but distinct, behavioral effects of FAAH and MAGL inhibitors raise provocative questions about the respective roles of anandamide and 2-AG in the nervous system. Several of the behavioral processes affected by FAAH inhibitors, including pain[12–15] and anxiety[12,25], contain a substantial component of stress. In contrast, MAGL inhibitors also appear to affect general neurological functions (for example, locomotor activity)[17,19]. Could these pharmacological profiles point to a broader role for 2-AG in the nervous system, with anandamide functioning as a more restricted, stress-responsive endocannabinoid? If so, what might be the effect of sustained elevations in anandamide and 2-AG on the integrity of the endocannabinoid system?

We found that prolonged pharmacological or genetic inactivation of MAGL caused profound alterations in the brain endocannabinoid system in mice, as evidenced by a loss of analgesic responses to a MAGL inhibitor, cross-tolerance to exogenous cannabinoid agonists, and CB_1 receptor downregulation and desensitization in specific brain regions. In contrast, none of these effects were observed in mice with chronically disrupted FAAH, which instead maintained an analgesic phenotype and intact CB_1 receptor system. Our results suggest that there are fundamental differences in the mode of signaling for

[1]Department of Pharmacology and Toxicology, Virginia Commonwealth University, Richmond, Virginia, USA. [2]The Skaggs Institute for Chemical Biology and Department of Chemical Physiology, The Scripps Research Institute, La Jolla, California, USA. [3]Department of Pharmacology and Toxicology, Medical College of Wisconsin, Milwaukee, Wisconsin, USA. [4]Department of Molecular Biology, The Scripps Research Institute, La Jolla, California, USA. [5]These authors contributed equally to this work. Correspondence should be addressed to A.H.L. (alichtma@vcu.edu) or B.F.C. (cravatt@scripps.edu).

Received 6 July; accepted 19 July; published online 22 August 2010; doi:10.1038/nn.2616

these two major endocannabinoid pathways in the nervous system that result in either sustained agonism or functional antagonism. That these effects occur through the same receptor (CB_1) suggests that ligand diversification is an important mechanism by which the endocannabinoid system modulates mammalian physiology and behavior.

RESULTS

Mouse models for chronic inactivation of MAGL

We established complementary pharmacological and genetic models to examine the consequences of sustained elevations in 2-AG in the nervous system. We generated a chronic pharmacological model by treating mice for six consecutive days with the MAGL inhibitor JZL184 (40 mg per kg of body weight, intraperitoneal, one dose per day), which has previously been shown to selectively inactivate MAGL in the nervous system and increase the level of 2-AG in the brain by up to tenfold that of control levels[17]. Mice treated with JZL184 acutely (single dose) or chronically showed highly elevated levels of 2-AG in the brain 2 h following final dosing (**Fig. 1a**). This increase in brain 2-AG levels persisted for at least 26 h (**Supplementary Fig. 1**), indicating that 2-AG remained elevated throughout the repeated dosing regime. Chronic, but not acute, dosing also caused a modest elevation in anandamide (~threefold) 2 h after final treatment (**Fig. 1a**), likely reflecting a partial blockade of FAAH[17] as a result of cumulative exposure to JZL184 over the treatment regimen. This change was, however, much lower than the 15-fold rise in brain anandamide that we observed in mice treated for 1 or 6 d with the selective FAAH inhibitor PF-3845 (10 mg per kg, intraperitoneal, one dose per day; **Fig. 1a**)[15] and was not of prolonged duration (**Supplementary Fig. 1**). PF-3845 did not alter brain 2-AG levels after acute or chronic treatment (**Fig. 1a**).

We also employed *Mgll*$^{-/-}$ mice as a complementary genetic model for sustained elevations in 2-AG. We obtained *Mgll*$^{-/-}$ mice generated by gene trapping from the Texas A&M Institute for Genomic Medicine (**Fig. 1b**,**c**) and confirmed by activity-based protein profiling[26,27] that these mice lack detectable MAGL activity without showing alterations in other brain serine hydrolase activities, including FAAH (**Fig. 1d** and **Supplementary Fig. 2**). We also confirmed the absence of MAGL expression in *Mgll*$^{-/-}$ mice by *in situ* hybridization and mass spectrometry–based proteomics (**Supplementary Fig. 3**). *Mgll*$^{-/-}$ mice exhibited marked (~90%) reductions in brain 2-AG hydrolytic activity (**Fig. 1e** and **Supplementary Fig. 2**) and about tenfold elevations in brain 2-AG levels (**Fig. 1f** and **Supplementary Table 1**). Brain arachidonic acid levels were also reduced in *Mgll*$^{-/-}$ mice (**Fig. 1f** and **Supplementary Table 1**) or mice treated acutely or chronically with JZL184 (**Supplementary Fig. 2**), consistent with previous findings designating 2-AG as a physiological precursor for arachidonic acid in the brain[17,28]. Anandamide levels were unaltered in *Mgll*$^{-/-}$ mice (**Fig. 1f** and **Supplementary Table 1**). We observed similar metabolic changes in a panel of peripheral tissues from JZL184-treated[29] or *Mgll*$^{-/-}$ mice, all of which showed reductions in 2-AG hydrolysis and elevations in 2-AG, but not anandamide (**Supplementary Fig. 4**). These data provide genetic confirmation that MAGL is the principal 2-AG hydrolase in the mouse brain and many peripheral tissues and establish *Mgll*$^{-/-}$ mice as a valid animal model for examining the neurophysiological and behavioral consequences of sustained elevations in 2-AG.

Chronic MAGL blockade causes tolerance in pain assays

Acute pharmacological blockade of MAGL or FAAH produced similar efficacy in multiple pain assays (**Fig. 2**), including antinociception in the acute thermal tail-withdrawal test (**Fig. 2a**) and reductions in mechanical (**Fig. 2b**) and cold (**Fig. 2c**) allodynia in the chronic constrictive injury of the sciatic nerve (CCI) model. In contrast, prolonged disruption of these enzymes resulted in a marked difference in the expression of tolerance. Although mice treated repeatedly with PF-3845 maintained hypoalgesic (**Fig. 2a**) and anti-allodynic

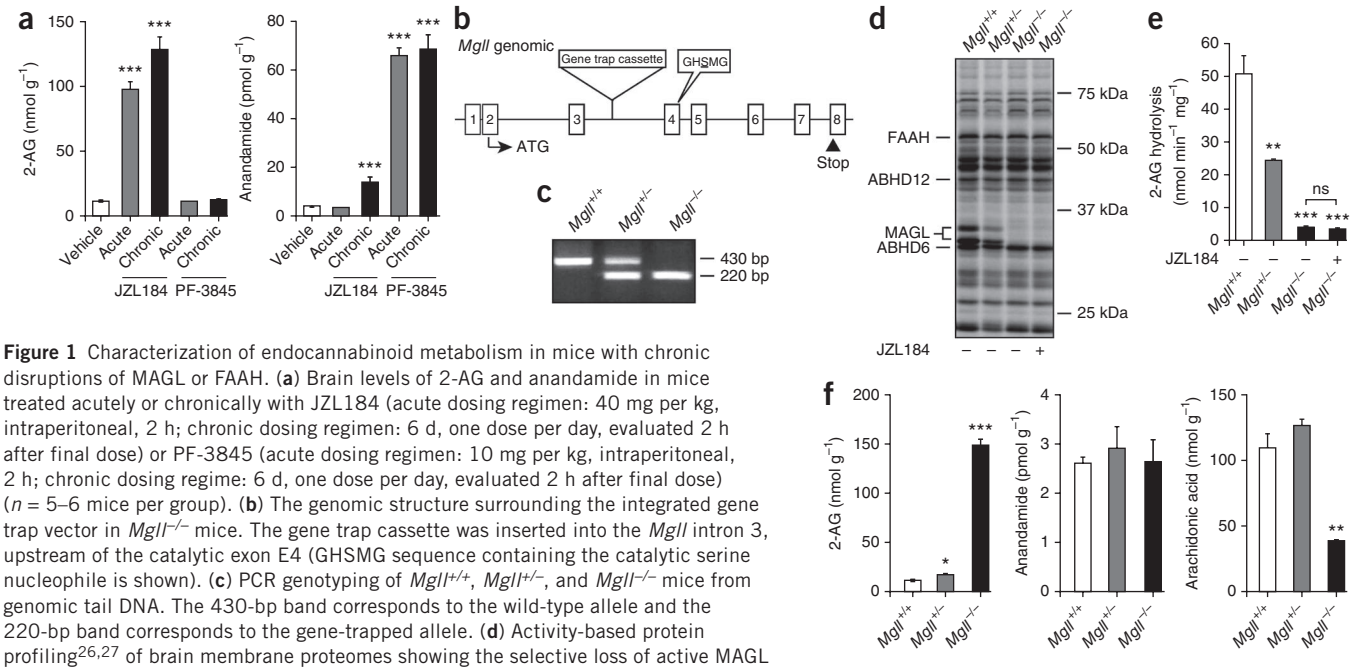

Figure 1 Characterization of endocannabinoid metabolism in mice with chronic disruptions of MAGL or FAAH. (**a**) Brain levels of 2-AG and anandamide in mice treated acutely or chronically with JZL184 (acute dosing regimen: 40 mg per kg, intraperitoneal, 2 h; chronic dosing regimen: 6 d, one dose per day, evaluated 2 h after final dose) or PF-3845 (acute dosing regimen: 10 mg per kg, intraperitoneal, 2 h; chronic dosing regime: 6 d, one dose per day, evaluated 2 h after final dose) (n = 5–6 mice per group). (**b**) The genomic structure surrounding the integrated gene trap vector in *Mgll*$^{-/-}$ mice. The gene trap cassette was inserted into the *Mgll* intron 3, upstream of the catalytic exon E4 (GHSMG sequence containing the catalytic serine nucleophile is shown). (**c**) PCR genotyping of *Mgll*$^{+/+}$, *Mgll*$^{+/-}$, and *Mgll*$^{-/-}$ mice from genomic tail DNA. The 430-bp band corresponds to the wild-type allele and the 220-bp band corresponds to the gene-trapped allele. (**d**) Activity-based protein profiling[26,27] of brain membrane proteomes showing the selective loss of active MAGL protein in *Mgll*$^{-/-}$ mice. (**e**) 2-AG hydrolytic activities of *Mgll*$^{+/+}$, *Mgll*$^{+/-}$ and *Mgll*$^{-/-}$ brain membrane proteomes (n = 4 per genotype). Note that treatment of the *Mgll*$^{-/-}$ brain proteome with JZL184 (5 μM) did not further decrease MAGL activity signals (**d**) or 2-AG hydrolysis (**e**), supporting the complete loss of MAGL in this sample. (**f**) Brain levels of 2-AG, anandamide and arachidonic acid from *Mgll*$^{+/+}$, *Mgll*$^{+/-}$ and *Mgll*$^{-/-}$ mice (n = 4–6 mice per genotype). Data are presented as means ± s.e.m. $^*P < 0.05$, $^{**}P < 0.01$ and $^{***}P < 0.001$ versus vehicle-treated (**a**) or wild-type littermate control mice (**e**,**f**) (Dunnett's *post hoc* test).

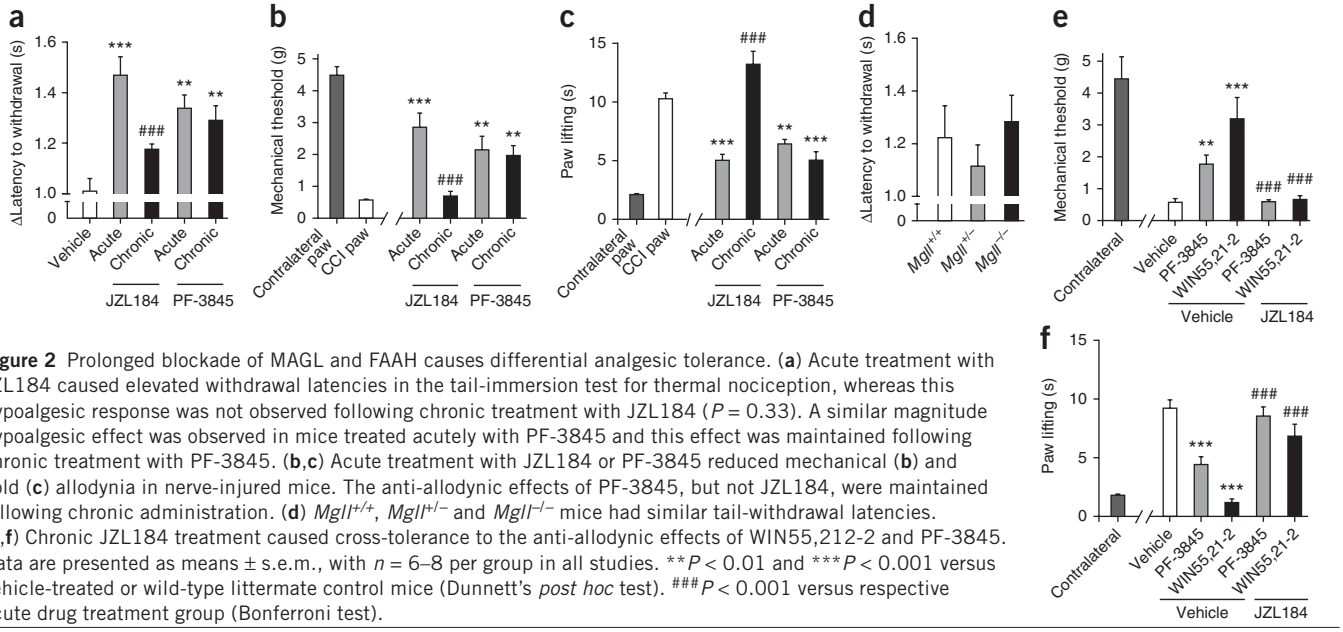

Figure 2 Prolonged blockade of MAGL and FAAH causes differential analgesic tolerance. (**a**) Acute treatment with JZL184 caused elevated withdrawal latencies in the tail-immersion test for thermal nociception, whereas this hypoalgesic response was not observed following chronic treatment with JZL184 ($P = 0.33$). A similar magnitude hypoalgesic effect was observed in mice treated acutely with PF-3845 and this effect was maintained following chronic treatment with PF-3845. (**b**,**c**) Acute treatment with JZL184 or PF-3845 reduced mechanical (**b**) and cold (**c**) allodynia in nerve-injured mice. The anti-allodynic effects of PF-3845, but not JZL184, were maintained following chronic administration. (**d**) *Mgll*$^{+/+}$, *Mgll*$^{+/-}$ and *Mgll*$^{-/-}$ mice had similar tail-withdrawal latencies. (**e**,**f**) Chronic JZL184 treatment caused cross-tolerance to the anti-allodynic effects of WIN55,212-2 and PF-3845. Data are presented as means ± s.e.m., with $n = 6$–8 per group in all studies. $^{**}P < 0.01$ and $^{***}P < 0.001$ versus vehicle-treated or wild-type littermate control mice (Dunnett's *post hoc* test). $^{###}P < 0.001$ versus respective acute drug treatment group (Bonferroni test).

(**Fig. 2b**,**c**) responses, mice chronically treated with JZL184 showed similar pain responses as control mice (**Fig. 2a**–**c**). Similarly, *Mgll*$^{-/-}$ mice displayed equivalent tail-withdrawal latencies as *Mgll*$^{+/+}$ and *Mgll*$^{+/-}$ mice (**Fig. 2d**).

These findings indicate that the analgesic effects produced by acute blockade of MAGL are lost following sustained inactivation of this enzyme. We next investigated whether this form of tolerance was a result of alterations in the endocannabinoid system.

Chronic MAGL blockade causes tolerance to CB_1 agonists

We assessed the behavioral effects of cannabinoid receptor agonists in mice with chronic disruptions in FAAH or MAGL. *Faah*$^{-/-}$ mice[10], as well as mice that were chronically treated with PF-3845 (**Supplementary Fig. 5**), exhibited wild-type responses to cannabinoids in antinociception, hypothermia and catalepsy assays, indicating that CB_1 function was normal. In contrast, *Mgll*$^{-/-}$ mice or mice treated chronically with JZL184 showed reduced responses to the antinociceptive and hypothermic effects of THC (**Supplementary Fig. 6**) and the full CB_1 agonist WIN55,212-2 (**Fig. 3**). Chronic JZL184 treatment also elicited marked cross-tolerance to the anti-allodynic effects of WIN55,212-2 and PF-3845 in the CCI model (**Fig. 2e**,**f**). CB_1 agonist-induced catalepsy was less affected by sustained inactivation of MAGL (**Fig. 3c**,**f** and **Supplementary Fig. 6**). These data indicate that sustained inactivation of MAGL causes cross-tolerance to exogenous CB_1 agonists and to a FAAH inhibitor in a neuropathic pain model.

We next asked whether prolonged MAGL or FAAH blockade produces physical dependence, a phenotype that has been observed in rodents that have been exposed to repeated treatments with direct CB_1 agonists[30]. The CB_1 receptor antagonist rimonabant precipitated paw flutters in mice that were chronically treated with JZL184 to a similar degree as mice subjected to a mild THC chronic dosing regimen (10 mg per kg per day for 6 d; **Supplementary Fig. 7**). In contrast, rimonabant did not precipitate paw tremors in mice that were chronically administered PF-3845.

Brain CB_1 receptors are impaired by chronic MAGL blockade

The loss of analgesic responses and occurrence of cannabinoid cross-tolerance in mice with sustained disruptions of MAGL suggested that CB_1 receptors might be downregulated and/or desensitized in these mice. In support of this hypothesis, brain tissue from *Mgll*$^{-/-}$ mice or mice chronically treated with JZL184 showed decreases in CB_1 receptor number and function, as measured by specific binding of

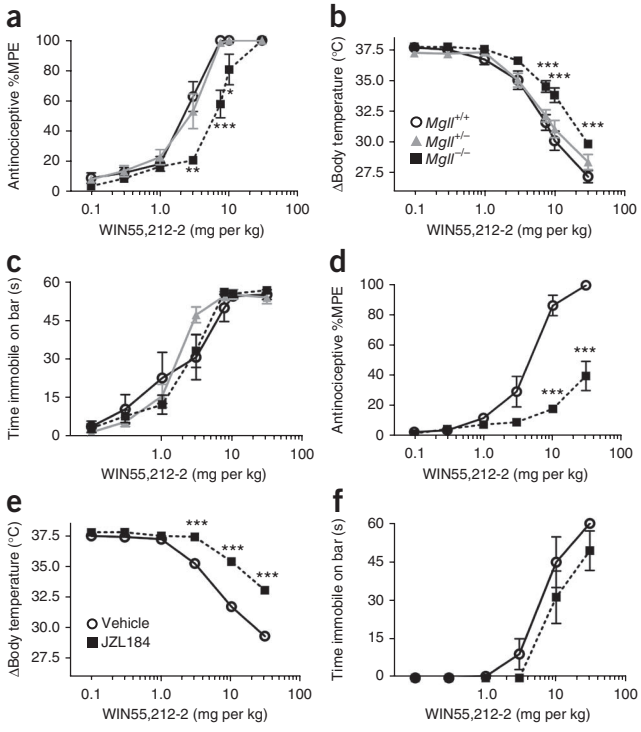

Figure 3 Chronic disruption of MAGL produces behavioral cross-tolerance to a subset of the pharmacological effects of the cannabinoid receptor agonist WIN55,212-2. (**a**–**c**) *Mgll*$^{-/-}$ mice showed significant cross-tolerance to the antinociceptive (**a**) and hypothermic (**b**), but not to the cataleptic (**c**), effects of WIN55,212-2. (**d**–**f**) Similarly, chronic treatment with JZL184 caused significant cross-tolerance to the antinociceptive (**d**) and hypothermic (**e**), but not the cataleptic (**f**), effects of WIN55,212-2. Data are presented as means ± s.e.m., $n = 7$–8 per group. $^{*}P < 0.05$, $^{**}P < 0.01$ and $^{***}P < 0.001$ versus vehicle-treated or wild-type littermate control mice (planned comparisons).

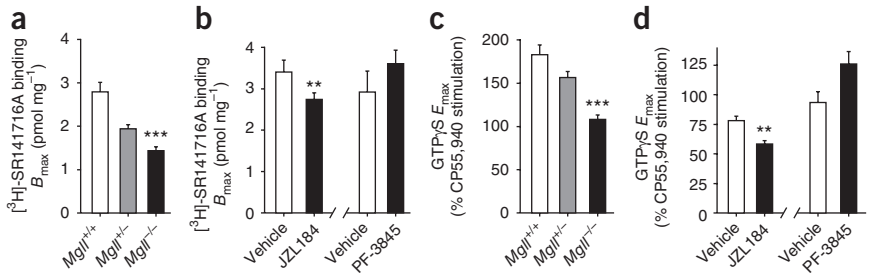

Figure 4 Chronic disruption of MAGL produces CB_1 receptor downregulation and desensitization in the mouse brain. (**a**,**b**) Comparison of the membrane-specific CB_1 receptor binding by the antagonist [^{3}H]-SR141716A, as evaluated by the best-fit B_{max} of binding curves from whole brain homogenates. *Mgll*$^{-/-}$ mice and mice treated chronically with JZL184, but not mice treated chronically with PF-3845, had significantly fewer CB_1 receptors. (**c**,**d**) CP55,940-stimulated [^{35}S]-GTPγS binding. *Mgll*$^{-/-}$ mice and mice treated chronically with JZL184, but not mice treated chronically with PF-3845, showed CB_1 receptor desensitization. Data are presented as means ± s.e.m. of nonlinear regression best-fit values of specific binding or sigmoidal dose-response curves ($n = 4$ tissue samples per group, run in separate experiments with each individual sample run in triplicate for GTPγS and duplicate for receptor binding). $^{**}P < 0.01$ and $^{***}P < 0.001$ versus vehicle-treated or wild-type littermate control mice (determined by regression confidence intervals).

^{3}H-rimonbabant (**Fig. 4a**,**b** and **Supplementary Fig. 8**) and CB_1 agonist (CP55,940)-stimulated [^{35}S] GTPS binding (**Fig. 4c**,**d** and **Supplementary Fig. 8**), respectively. In contrast, prolonged blockade of FAAH by PF-3845 did not affect CB_1 receptor expression or function (**Fig. 4b**,**d** and **Supplementary Fig. 8**). These findings are consistent with previous work showing that CB_1 receptor numbers and function are not altered in *Faah*$^{-/-}$ mice[31,32].

To provide further evidence that the behavioral tolerance and CB_1 receptor adaptations caused by chronic MAGL blockade were the results of elevated 2-AG acting on CB_1 receptors (as opposed to other metabolic alterations, such as reductions in arachidonic acid), we attempted to block these changes by concurrent chronic treatment with rimonabant. For technical reasons, we focused on antinociception for our behavioral measurements (**Supplementary Discussion**). Over a 6-d period, we treated mice daily with vehicle, JZL184 (40 mg per kg, intraperitoneal), rimonabant (3 mg per kg, intraperitoneal), or both JZL184 (40 mg per kg, intraperitoneal) and rimonabant (3 mg per kg, intraperitoneal), yielding four treatment groups. As shown previously (**Fig. 3**), chronic JZL184–treated mice produced marked tolerance to the anti-nociceptive effects of WIN55,212-2 (**Supplementary Fig. 9**). In contrast, the rimonabant-JZL184–treated mice exhibited greater antinociceptive responses to WIN55,212-2 that were close in magnitude to those observed in control (vehicle or rimonabant) mice (**Supplementary Fig. 9**). These data indicate that daily treatment with rimonabant substantially prevents the nociceptive adaptations caused by chronic MAGL blockade. Rimonabant treatment (10 mg per kg, intraperitoneal) also ameliorated brain CB_1 receptor adaptations in chronic JZL184–treated mice, as determined by CP55,940-stimulated [^{35}S]-GTPγS binding (**Supplementary Fig. 9**).

A more extensive regional analysis of CP55,940-stimulated [^{35}S]GTPγS binding in mice treated chronically with either vehicle or JZL184 revealed that sustained MAGL blockade produced a heterogeneous reduction in CB_1 function throughout the brain (**Fig. 5**). Notable brain regions showing CB_1 desensitization included the cingulate cortex, hippocampus, somatosensory cortex and PAG (**Fig. 5b**). In contrast, chronic JZL184 treatment did not elicit desensitization in the caudate putamen or globus pallidus. These data, taken together, indicate that prolonged inactivation of MAGL, but not FAAH, causes marked changes in CB_1 receptor expression and function in specific brain regions, including those that participate in pain perception (for example, the PAG) and cognitive/emotional processing of pain[33] (for example, cingulate cortex).

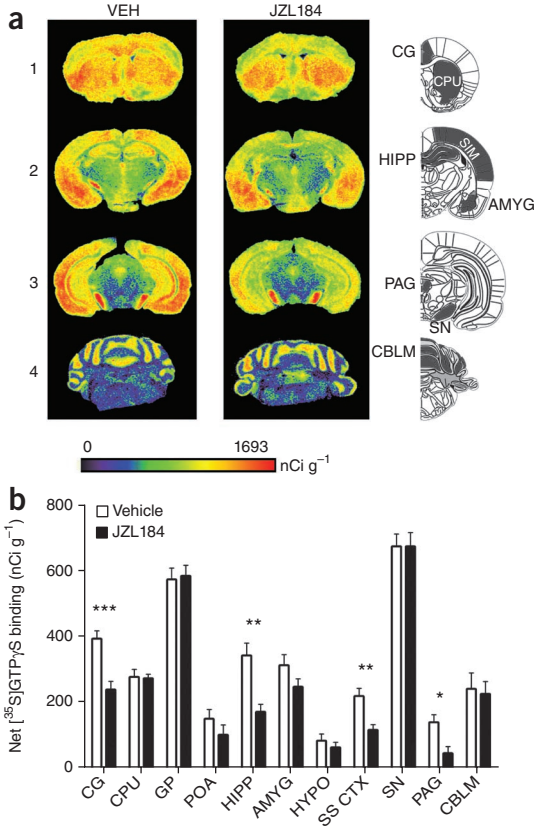

Figure 5 Regional changes in cannabinoid agonist–stimulated [^{35}S]GTPγS binding following chronic disruption of MAGL. (**a**) Representative autoradiograms showing CP55,940-stimulated [^{35}S] GTPγS binding in coronal brain sections following either chronic vehicle (left) or JZL184 (right) treatment. Pseudocolor images indicate levels of receptor-mediated G protein activity and highlight decreases in CB_1 receptor activation in the cingulate cortex (CG, row 1), hippocampus (HIPP, row 2) and periaqueductal gray (PAG, row 3). No differences were apparent in the caudate putamen (CPU, row 1) or cerebellum (CBLM, row 4). (**b**) Densitometric analysis of CP55,940-stimulated [^{35}S]GTPγS binding in selected regions, including cingulate cortex, caudate putamen, globus pallidus (GP), preoptic area of the hypothalamus (POA), hippocampus, amygdala (AMYG), hypothalamus (HYPO), somatosensory cortex (SS CTX), substantia nigra (SN), periaqueductal gray and cerebellum. Data are presented as means ± s.e.m., $n = 8$ brains per group, run in triplicate slices for each targeted region. $^{*}P < 0.05$, $^{**}P < 0.01$ and $^{***}P < 0.001$ versus vehicle treatment for specific region (Student's t test).

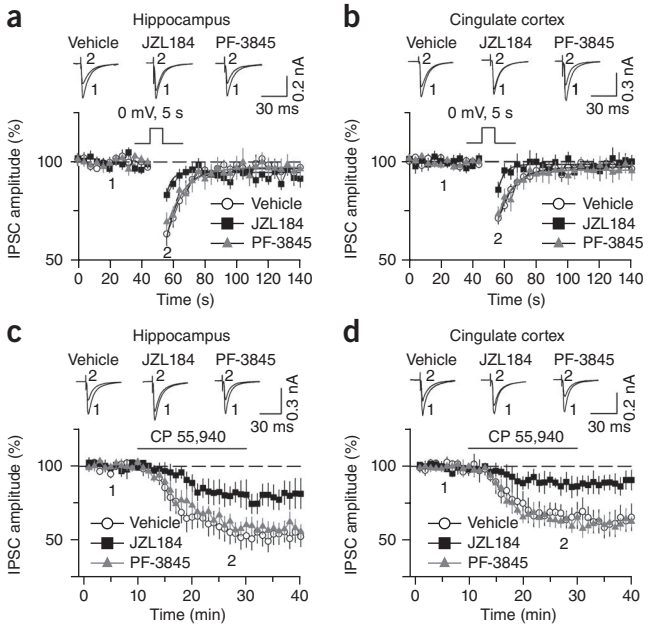

Figure 6 Chronic disruption of MAGL impairs CB_1-dependent forms of synaptic plasticity. (**a**,**b**) Chronic treatment with JZL184, but not PF-3845, attenuated DSI in hippocampal CA1 pyramidal neurons (**a**) and layer V pyramidal neurons of the cingulate cortex (**b**) ($P < 0.01$ for JZL184- versus vehicle-treated groups for both magnitude and τ of DSI, $n = 11$–15 mice per group). The lines superimposed are the single exponential fitting curves of the decay of DSI. (**c**,**d**) Bath application of the CB_1 agonist CP55,940 (3 μM) induced significantly less depression of IPSCs in the hippocampus (**c**) and cingulate cortex (**d**) from mice chronically treated with JZL184 than in those from vehicle-treated control mice ($P < 0.05$ in both brain regions). Brain regions from mice chronically treated with PF-3845 did not differ significantly from vehicle controls ($P > 0.05$; $n = 6$–7 mice per group). Data are presented as means ± s.e.m.

Synaptic plasticity is impaired by chronic MAGL blockade

Endocannabinoids regulate several forms of synaptic plasticity[34], including DSI in the hippocampus[20]. Considering that CB_1 receptors were impaired in this brain region by sustained MAGL inactivation, we asked whether DSI was also affected. In contrast with previous findings that acute inhibition of MAGL by bath application of JZL184 potentiates DSI in mouse hippocampal slices[20], we observed decreases in the magnitude and time constant (τ) of DSI in hippocampal slices from mice chronically treated with JZL184 when compared with slices from vehicle-treated mice (**Fig. 6a**). We observed similar effects in layer V pyramidal neurons of the cingulate cortex, where acute (**Supplementary Fig. 10**) and chronic (**Fig. 6b**) treatment with JZL184 potentiated and disrupted DSI, respectively. PF-3845 did not affect DSI in the hippocampus (**Fig. 6a**) or cingulate cortex (**Fig. 6b** and **Supplementary Fig. 10**).

The attenuation of DSI by chronic JZL184 treatment is consistent with desensitization of CB_1 receptors in the affected neuronal circuits (**Fig. 5**). In support of this premise, CP55,940 (3 μM) induced less depression of inhibitory postsynaptic currents (IPSCs) in the hippocampal CA1 pyramidal neurons or layer V pyramidal neurons of the cingulate cortex from chronically JZL184–treated mice than in those from vehicle-treated mice (**Fig. 6c**,**d**). In contrast, repeated *in vivo* administration of PF-3845 did not alter CP55,940-induced depression of IPSCs in either hippocampus (**Fig. 6c**) or cingulate cortex (**Fig. 6d**). The CB_1 receptor antagonist AM251 (2 μM) completely blocked CP55,940-induced depression of IPSCs in both brain regions (**Supplementary Fig. 11**). Notably, chronic JZL184 treatment exerted only a modest effect that did not reach statistical significance ($P > 0.05$) on CP55,940-induced depression of IPSCs in the caudate putamen (**Supplementary Fig. 12**), a brain region that also showed minimal CB_1 receptor adaptations (**Fig. 5**).

Recent studies have suggested that CB_1 receptors on glutamatergic synapses mediate many of the behavioral effects of CB_1 agonists[35]. We therefore examined whether chronic JZL184 or PF-3845 treatment altered CB_1-mediated depression of glutamatergic excitatory transmission in the hippocampus. Chronic JZL184, but not PF-3845, treatment attenuated CP55,940-induced depression of field excitatory postsynaptic potentials (fEPSPs) in the CA1 region of the hippocampus (**Supplementary Fig. 13**).

These results, taken together, indicate that sustained inactivation of MAGL, but not FAAH, impairs specific endocannabinoid-mediated forms of synaptic plasticity. That we observed these effects for both glutamatergic and GABAergic transmission is consistent with previous findings that acute MAGL, but not FAAH, blockade enhances both DSE and DSI[20] and that diacylglycerol lipase-α knockout mice exhibit defects in both DSE and DSI[23,24].

DISCUSSION

Prolonged treatment with THC and other cannabinoid receptor agonists leads to the development of tolerance and physical dependence[36] and these behavioral phenotypes have been shown to be mirrored by substantial reductions in CB_1 receptor expression and activity in the brain[37,38]. We found that sustained elevations in brain 2-AG caused by either genetic deletion or chronic pharmacological blockade of MAGL also produced substantial functional antagonism of the brain endocannabinoid system, as manifested by tolerance to the analgesic effects of acute enzyme inhibition, cross-tolerance to CB_1 receptor agonists, a reduction in CB_1 receptor expression and function, and disruptions in endocannabinoid-dependent synaptic plasticity. This profile markedly contrasted with that of sustained pharmacological disruption of FAAH, which caused persistent analgesic effects without evidence of tolerance or changes in CB_1 receptor expression or function. Thus, brain CB_1 receptors undergo markedly different adaptations in response to sustained elevations of the two principal endocannabinoids, 2-AG and anandamide.

That the cannabinoid cross-tolerance and alterations in CB_1 receptor function caused by JZL184 were both attenuated by co-treatment with rimonabant supports a model in which chronic MAGL blockade produces a sustained elevation in 2-AG that tonically activates and eventually desensitizes CB_1 receptors in the brain. We cannot, however, rule out the possibility that other metabolic changes caused by MAGL inhibition, such as reductions in arachidonic acid, also contribute to alterations in brain endocannabinoid pathways. We also note that chronic JZL184 treatment produced an evidently larger degree of cross-tolerance to CB_1 agonists (**Fig. 3a**,**b**) than genetic disruption of *Mgll* (**Fig. 3d**,**e**). Although we do not yet understand the basis for this difference, it could reflect differences in background strain (C57BL/6J versus 129SvEv/C57BL/6J for the JZL184-treated and $Mgll^{-/-}$ mice, respectively) or the existence of compensatory mechanisms in the $Mgll^{-/-}$ mice that counteract the observed CB_1 receptor adaptations.

Although there are other examples of functional antagonism of receptor systems following deletion of a metabolic enzyme, including reduced activity of nicotinic receptors[39] in $Ache^{-/-}$ (*acetylcholinesterase*) mice and impairments in 5-HT1A receptors in $Maoa^{-/-}$ (*monoamine oxidase A*) mice[40], we report the first instance, to the best of our

knowledge, in which disruption of an enzyme that degrades a lipid transmitter leads to receptor downregulation and desensitization in the nervous system. This finding indicates that, despite fundamental differences in the mechanisms of storage and release (vesicular versus nonvesicular), classical neurotransmitters and lipid messengers are both capable of causing tolerance and receptor desensitization following chronic inactivation of their cognate degradative enzymes. That behavioral and CB_1 receptor adaptations occurred only in mice with chronically inactivated MAGL, but not FAAH, indicates that sustained elevations in 2-AG exert a greater effect than anandamide on the integrity of the brain endocannabinoid system. How 2-AG is more capable of causing substantial CB1 alterations *in vivo* remains unclear, but our data would indicate that this effect is not necessarily correlated with the induction of superior efficacy in behavioral assays. Indeed, MAGL and FAAH inhibitors displayed similar relative analgesic activity in acute treatment procedures. One possibility is that 2-AG and anandamide have differential effects on CB_1 receptor desensitization and/or recycling in the brain, as has been observed previously in heterologous expression systems[41]. This differential desensitization may be related to the higher efficacy of 2-AG as a full CB_1 receptor agonist (in contrast with anandamide, which acts as a partial CB_1 receptor agonist)[42], although previous research suggests that the magnitude of CB_1 receptor desensitization is not related to the intrinsic activity of exogenous agonists[43]. Bulk brain levels of 2-AG are also much higher than anandamide (see **Fig. 1a**; although the interstitial levels of these endocannabinoid are similar[44]), and elevated 2-AG may therefore achieve greater occupancy of CB_1 receptors *in vivo*. Finally, MAGL and FAAH are found in different neuronal populations and subcellular compartments (pre- and postsynaptic, respectively) throughout the brain and these anatomical distinctions might also differentially affect endocannabinoid signaling pathways in the nervous system. Regardless, our observation that chronic MAGL blockade produced cross-tolerance to a FAAH inhibitor in the CCI model (**Fig. 2e**,**f**) indicates that 2-AG and anandamide pathways can crosstalk in the neural circuits that regulate pain behavior.

The endocannabinoid system regulates several forms of synaptic plasticity, including DSI and DSE[34]. Acute MAGL, but not FAAH, inhibition potentiates DSI in neurons of the hippocampus[20] and cingulate cortex (**Supplementary Fig. 4**). Notably, however, we found that repeated administration of JZL184 led to profound DSI deficits in these neuronal populations (**Fig. 6**). These impairments in short-term synaptic plasticity are consistent with the observed alterations in CB_1 receptor function in the hippocampus and cingulate cortex (**Fig. 5**), as deletion or antagonism of this receptor has been shown to abolish DSI[22,45]. That acute and chronic inhibition of MAGL produced opposing effects on DSI in multiple brain regions supports a model in which prolonged elevations of endogenous 2-AG cause functional antagonism of CB_1 receptors in the nervous system.

In contrast with direct CB_1 agonists, which produce cross-tolerance to the antinociceptive, hypothermic and cataleptic effects of THC and WIN55,212-2 (ref. 46), chronic MAGL disruption only caused strong cross-tolerance to the antinociceptive and hypothermic effects of these drugs. The minimal cross-tolerance to cannabinoid-induced catalepsy is consistent with the lack of CB_1 receptor desensitization in caudate putamen and globus pallidus (**Fig. 5**), which are associated with cannabinoid-induced catalepsy[47]. Conversely, the tolerance that we observed to the antinociceptive effects of JZL184 and the occurrence of cross-tolerance to WIN55,212-2– and THC-induced antinociception could be attributed to the desensitization of CB_1 receptors in PAG (**Fig. 5**), a brain area that has been strongly implicated in cannabinoid-induced antinociception[48]. We also note that neither MAGL nor FAAH inhibitors alone cause catalepsy; however, combined treatment with these inhibitors does promote cataleptic behavioral responses[19]. It will be interesting to determine whether sustained inactivation of both MAGL and FAAH causes cross-tolerance to the cataleptic effects of other CB_1 agonists and concomitant alterations in CB_1 receptor expression and activity in brain regions such as the caudate putamen and globus pallidus.

In summary, our data support a model in which ligand diversification is important for shaping the distinct functions and properties of endocannabinoid signaling pathways in the nervous system. The widespread behavioral and CB_1 receptor adaptations caused by chronic disruption of MAGL suggest a broad role for 2-AG throughout the nervous system. In contrast, the preservation of analgesic phenotypes and CB_1 receptor function in mice with sustained inactivation of FAAH may reflect a more limited, stress-dependent function for anandamide. This idea is also consistent with the behavioral phenotypes observed in FAAH-disrupted animals, which preferentially show reductions in pain[11] and anxiety[25] procedures with strong stress components. These discoveries may have important translational implications. Consider, for instance, that acute inhibition of FAAH and MAGL produces similar efficacy in multiple pain assays, but these effects are only sustained in chronically disrupted FAAH systems. Might this imply that MAGL is a less suitable target for treatment of pain disorders? Perhaps, but it also may be possible to achieve prolonged analgesic responses through partial MAGL blockade. In this event, one would still need to be concerned about the potential tolerance and withdrawal effects of MAGL inhibitors. That CB_1 receptors, on the other hand, are surprisingly nonadaptive to continuous elevations of brain anandamide suggests that FAAH inhibitors are capable of producing sustained analgesic activity without high risk for dependence.

METHODS

Methods and any associated references are available in the online version of the paper at http://www.nature.com/natureneuroscience/.

Note: Supplementary information is available on the Nature Neuroscience website.

ACKNOWLEDGMENTS

We thank S. Niessen and H. Hoover for assistance with proteomics studies, I. Beletskaya and R. Abdullah for technical support and the Cravatt and Lichtman laboratories for critical reading of the manuscript. This work was supported by the US National Institutes of Health (grants DA017259, DA009789, DA025285, DA005274, DA015683, DA03672, DA005274, DA07027, DA014277, DA023758 and DA024741), Ruth L. Kirschstein US National Institutes of Health Predoctoral Fellowships (DA026261 to J.L.B., DA026279 to J.E.S., DA028333 to L.B. and DA023758 to P.T.N.), the American Cancer Society (D.K.N.) and the Skaggs Institute for Chemical Biology.

AUTHOR CONTRIBUTIONS

J.E.S. performed behavioral and receptor adaptation experiments. J.L.B. performed the metabolic biochemistry, proteomic and *in situ* hybridization experiments and contributed to behavioral experiments. J.Z.L. contributed to metabolic biochemistry and behavioral experiments. D.K.N., S.G.K., D.R. and L.B. contributed to behavioral experiments. B.P. performed the electrophysiology experiments. P.T.N. and J.J.B. contributed to receptor adaptation experiments. E.A.T. contributed to the design and interpretation of *in situ* hybridization experiments. D.E.S and L.J.S.-S. contributed to the design and interpretation of receptor adaptation experiments. Q.-s.L. contributed to the design and interpretation of electrophysiology experiments. A.H.L. and B.F.C. supervised the design, execution and interpretation of the experiments and wrote the manuscript.

COMPETING FINANCIAL INTERESTS

The authors declare no competing financial interests.

Published online at http://www.nature.com/natureneuroscience/.
Reprints and permissions information is available online at http://www.nature.com/reprintsandpermissions/.

1. Pacher, P., Bátkai, S. & Kunos, G. The endocannabinoid system as an emerging target of pharmacotherapy. *Pharmacol. Rev.* **58**, 389–462 (2006).
2. Devane, W.A. *et al.* Isolation and structure of a brain constituent that binds to the cannabinoid receptor. *Science* **258**, 1946–1949 (1992).
3. Mechoulam, R. *et al.* Identification of an endogenous 2-monoglyceride, present in canine gut, that binds cannabinoid receptors. *Biochem. Pharmacol.* **50**, 83–90 (1995).
4. Sugiura, T. *et al.* 2-Arachidonylglycerol: a possible endogenous cannabinoid receptor ligand in brain. *Biochem. Biophys. Res. Commun.* **215**, 89–97 (1995).
5. Mackie, K. Cannabinoid receptors as therapeutic targets. *Annu. Rev. Pharmacol. Toxicol.* **46**, 101–122 (2006).
6. Marsicano, G. *et al.* CB1 cannabinoid receptors and on-demand defense against excitotoxicity. *Science* **302**, 84–88 (2003).
7. Fowler, C.J. The cannabinoid system and its pharmacological manipulation–a review, with emphasis upon the uptake and hydrolysis of anandamide. *Fundam. Clin. Pharmacol.* **20**, 549–562 (2006).
8. Ahn, K., McKinney, M.K. & Cravatt, B.F. Enzymatic pathways that regulate endocannabinoid signaling in the nervous system. *Chem. Rev.* **108**, 1687–1707 (2008).
9. Deutsch, D.G. & Chin, S.A. Enzymatic synthesis and degradation of anandamide, a cannabinoid receptor agonist. *Biochem. Pharmacol.* **46**, 791–796 (1993).
10. Cravatt, B.F. *et al.* Supersensitivity to anandamide and enhanced endogenous cannabinoid signaling in mice lacking fatty acid amide hydrolase. *Proc. Natl. Acad. Sci. USA* **98**, 9371–9376 (2001).
11. Lichtman, A.H., Shelton, C.C., Advani, T. & Cravatt, B.F. Mice lacking fatty acid amide hydrolase exhibit a cannabinoid receptor–mediated phenotypic hypoalgesia. *Pain* **109**, 319–327 (2004).
12. Kathuria, S. *et al.* Modulation of anxiety through blockade of anandamide hydrolysis. *Nat. Med.* **9**, 76–81 (2003).
13. Lichtman, A.H. *et al.* Reversible inhibitors of fatty acid amide hydrolase that promote analgesia: evidence for an unprecedented combination of potency and selectivity. *J. Pharmacol. Exp. Ther.* **311**, 441–448 (2004).
14. Jhaveri, M.D., Richardson, D., Kendall, D.A., Barrett, D.A. & Chapman, V. Analgesic effects of fatty acid amide hydrolase inhibition in a rat model of neuropathic pain. *J. Neurosci.* **26**, 13318–13327 (2006).
15. Ahn, K. *et al.* Discovery and characterization of a highly selective FAAH inhibitor that reduces inflammatory pain. *Chem. Biol.* **16**, 411–420 (2009).
16. Cravatt, B.F. *et al.* Molecular characterization of an enzyme that degrades neuromodulatory fatty-acid amides. *Nature* **384**, 83–87 (1996).
17. Long, J.Z. *et al.* Selective blockade of 2-arachidonoylglycerol hydrolysis produces cannabinoid behavioral effects. *Nat. Chem. Biol.* **5**, 37–44 (2009).
18. Kinsey, S.G. *et al.* Blockade of endocannabinoid-degrading enzymes attenuates neuropathic pain. *J. Pharmacol. Exp. Ther.* **330**, 902–910 (2009).
19. Long, J.Z. *et al.* Dual blockade of FAAH and MAGL identifies behavioral processes regulated by endocannabinoid crosstalk *in vivo*. *Proc. Natl. Acad. Sci. USA* **106**, 20270–20275 (2009).
20. Pan, B. *et al.* Blockade of 2-arachidonoylglycerol hydrolysis by selective monoacylglycerol lipase inhibitor 4-nitrophenyl 4-(dibenzo[d][1,3]dioxol-5-yl(hydroxy)methyl) piperidine-1-carboxylate (JZL184) enhances retrograde endocannabinoid signaling. *J. Pharmacol. Exp. Ther.* **331**, 591–597 (2009).
21. Straiker, A. *et al.* Monoacylglycerol lipase limits the duration of endocannabinoid-mediated depolarization-induced suppression of excitation in autaptic hippocampal neurons. *Mol. Pharmacol.* **76**, 1220–1227 (2009).
22. Wilson, R.I. & Nicoll, R.A. Endocannabinoid signaling in the brain. *Science* **296**, 678–682 (2002).
23. Tanimura, A. *et al.* The endocannabinoid 2-arachidonoylglycerol produced by diacylglycerol lipase alpha mediates retrograde suppression of synaptic transmission. *Neuron* **65**, 320–327 (2010).
24. Gao, Y. *et al.* Loss of retrograde endocannabinoid signaling and reduced adult neurogenesis in diacylglycerol lipase knock-out mice. *J. Neurosci.* **30**, 2017–2024 (2010).
25. Haller, J. *et al.* Interactions between environmental aversiveness and the anxiolytic effects of enhanced cannabinoid signaling by FAAH inhibition in rats. *Psychopharmacology (Berl.)* **204**, 607–616 (2009).
26. Liu, Y., Patricelli, M.P. & Cravatt, B.F. Activity-based protein profiling: the serine hydrolases. *Proc. Natl. Acad. Sci. USA* **96**, 14694–14699 (1999).
27. Blankman, J.L., Simon, G.M. & Cravatt, B.F. A comprehensive profile of brain enzymes that hydrolyze the endocannabinoid 2-arachidonoylglycerol. *Chem. Biol.* **14**, 1347–1356 (2007).
28. Nomura, D.K. *et al.* Activation of the endocannabinoid system by organophosphorus nerve agents. *Nat. Chem. Biol.* **4**, 373–378 (2008).
29. Long, J.Z., Nomura, D.K. & Cravatt, B.F. Characterization of monoacylglycerol lipase inhibition reveals differences in central and peripheral endocannabinoid metabolism. *Chem. Biol.* **16**, 744–753 (2009).
30. Aceto, M.D., Scates, S.M., Lowe, J.A. & Martin, B.R. Cannabinoid precipitated withdrawal by the selective cannabinoid receptor antagonist, SR 141716A. *Eur. J. Pharmacol.* **282**, R1–R2 (1995).
31. Falenski, K.W. *et al.* *Faah*$^{-/-}$ mice display differential tolerance, dependence and cannabinoid receptor adaptation following Δ9-tetrahydrocannabinol and anandamide administration. *Neuropsychopharmacology* **35**, 1775–1787 (2010).
32. Lichtman, A.H., Hawkins, E.G., Griffin, G. & Cravatt, B.F. Pharmacological activity of fatty acid amides is regulated, but not mediated, by fatty acid amide hydrolase *in vivo*. *J. Pharmacol. Exp. Ther.* **302**, 73–79 (2002).
33. Wilson, R.I., Kunos, G. & Nicoll, R.A. Presynaptic specificity of endocannabinoid signaling in the hippocampus. *Neuron* **31**, 453–462 (2001).
34. Kreitzer, A.C. & Regehr, W.G. Retrograde signaling by endocannabinoids. *Curr. Opin. Neurobiol.* **12**, 324–330 (2002).
35. Monory, K. *et al.* Genetic dissection of behavioural and autonomic effects of Δ9-tetrahydrocannabinol in mice. *PLoS Biol.* **5**, e269 (2007).
36. Lichtman, A.H. & Martin, B.R. Cannabinoid tolerance and dependence. *Handb. Exp. Pharmacol.* **168**, 691–717 (2005).
37. Sim, L.J., Hampson, R.E., Deadwyler, S.A. & Childers, S.R. Effects of chronic treatment with Δ9-tetrahydrocannabinol on cannabinoid-stimulated [35S]GTPγS autoradiography in rat brain. *J. Neurosci.* **16**, 8057–8066 (1996).
38. Romero, J. *et al.* Effects of chronic exposure to Δ9-tetrahydrocannabinol on cannabinoid receptor binding and mRNA levels in several rat brain regions. *Brain Res. Mol. Brain Res.* **46**, 100–108 (1997).
39. Sun, M., Lee, C.J. & Shin, H.S. Reduced nicotinic receptor function in sympathetic ganglia is responsible for the hypothermia in the acetylcholinesterase knockout mouse. *J. Physiol. (Lond.)* **578**, 751–764 (2007).
40. Lanoir, J., Hilaire, G. & Seif, I. Reduced density of functional 5-HT1A receptors in the brain, medulla and spinal cord of monoamine oxidase-A knockout mouse neonates. *J. Comp. Neurol.* **495**, 607–623 (2006).
41. Luk, T. *et al.* Identification of a potent and highly efficacious, yet slowly desensitizing CB1 cannabinoid receptor agonist. *Br. J. Pharmacol.* **142**, 495–500 (2004).
42. Hillard, C.J. Biochemistry and pharmacology of the endocannabinoids arachidonylethanolamide and 2-arachidonylglycerol. *Prostaglandins Other Lipid Mediat.* **61**, 3–18 (2000).
43. Sim-Selley, L.J. & Martin, B.R. Effect of chronic administration of R-(+)-[2,3-dihydro-5-methyl-3-[(morpholinyl)methyl]pyrrolo[1,2,3-de]-1,4-b enzoxazinyl]-(1-naphthalenyl)methanone mesylate (WIN55,212–2) or Δ9-tetrahydrocannabinol on cannabinoid receptor adaptation in mice. *J. Pharmacol. Exp. Ther.* **303**, 36–44 (2002).
44. Caillé, S., Alvarez-Jaimes, L., Polis, I., Stouffer, D.G. & Parsons, L.H. Specific alterations of extracellular endocannabinoid levels in the nucleus accumbens by ethanol, heroin and cocaine self-administration. *J. Neurosci.* **27**, 3695–3702 (2007).
45. Ohno-Shosaku, T., Maejima, T. & Kano, M. Endogenous cannabinoids mediate retrograde signals from depolarized postsynaptic neurons to presynaptic terminals. *Neuron* **29**, 729–738 (2001).
46. Fan, F., Compton, D.R., Ward, S., Melvin, L. & Martin, B.R. Development of cross-tolerance between Δ9-tetrahydrocannabinol, CP 55,940 and WIN 55,212. *J. Pharmacol. Exp. Ther.* **271**, 1383–1390 (1994).
47. Pertwee, R.G. & Wickens, A.P. Enhancement by chlordiazepoxide of catalepsy induced in rats by intravenous or intrapallidal injections of enantiomeric cannabinoids. *Neuropharmacology* **30**, 237–244 (1991).
48. Lichtman, A.H., Cook, S.A. & Martin, B.R. Investigation of brain sites mediating cannabinoid-induced antinociception in rats: evidence supporting periaqueductal gray involvement. *J. Pharmacol. Exp. Ther.* **276**, 585–593 (1996).

ONLINE METHODS

Animals. Subjects consisted of male C57BL/6J mice (Jackson Laboratories) as well as male and female *Mgll*$^{+/+}$, *Mgll*$^{+/-}$ and *Mgll*$^{-/-}$ mice on a mixed 129SvEv/C57BL/6J background. *Mgll*$^{Gt1(neo)}$ mutant mice (TG0078; derived from OmniBank ES cell line OST113734) containing a gene trap vector inserted into the third intron of the *Mgll* gene were obtained from the Texas Institute of Genomic Medicine. The gene trap vector insertion site was mapped to the sequence GCC TTG TGG ACT GGA T(gene trap insertion)CT TGG GCC TTC TGT TC, which is upstream of the *Mgll* catalytic exon 4. *Mgll* genotype was determined by PCR amplification of genomic tail DNA using the following primers designed by Texas Institute of Genomic Medicine: *Mgll* forward 5′-TTG CCT GCT TGC TCT TAA CTC TTG C-3′, *Mgll* reverse 5′-GGG AGT CAA GAC ACT GGG GAA TCC T-3′, and gene trap reverse 5′-ATA AAC CCT CTT GCA GTT GCA TC-3′, which amplified a 430-bp product for the wild-type allele and a 220-bp product for the gene-trapped allele. Mice homozygous for the gene-trap (*Mgll*$^{-/-}$ mice) are viable, born at the expected Mendelian frequency, and display normal cage behavior compared with *Mgll*$^{+/+}$ and *Mgll*$^{-/-}$ littermates. Animal experiments were conducted in accordance with the guidelines of the Institutional Animal Care and Use Committees of the Scripps Research Institute and Virginia Commonwealth University.

Drugs and chemicals. JZL184 and PF-3845 were synthesized as described previously[15,17]. WIN55,212 was purchased from Cayman Chemical. Rimonabant, THC and CP55,940 were obtained from the Drug Supply Program of the National Institute on Drug Abuse. AM251 was obtained from Tocris. GDP, GTPγS, adenosine deaminase and bovine serum albumin (BSA) were purchased from Sigma-Aldrich. [^{35}S]GTPγS (1250 Ci mmol^{-1}) was obtained from PerkinElmer Life and Analytical Sciences. [^{3}H]SR141716A (44.0 Ci mmol^{-1}) was purchased from Amersham Pharmacia. Scintillation fluid (ScinitSafe Econo 1) was purchased from Thermo Fisher Scientific and Whatman GF/B glass fiber filters were obtained through Fisher Scientific.

Drugs were dissolved via sonification in a vehicle consisting of ethanol, Alkamuls-620 (Sanofi-aventis) and saline in a ratio of 1:1:18. All drugs were administered via the intraperitoneal route of administration in a volume of 10 µl per g of body mass. For chronic drug administration, subjects received a daily injection of JZL184 (40 mg per kg), PF-3845 (10 mg per kg), THC (10 mg per kg), rimonabant (3 mg per kg for behavioral analysis, 10 mg per kg for CB_1 receptor adaptation) or vehicle for 6 d.

Preparation of mouse brain homogenates. Membrane and soluble brain homogenates from C57BL6/J and *Mgll*$^{+/+}$, *Mgll*$^{+/-}$ and *Mgll*$^{-/-}$ mice (n = 4 per genotype) were prepared as previously described[29].

Activity-based protein profiling analysis. Analysis of brain proteomes pretreated with 5 µM JZL184 or DMSO vehicle (30 min at 25 °C) was performed as described previously[27].

2-AG hydrolysis assays. 2-AG hydrolytic activity of *Mgll*$^{+/+}$, *Mgll*$^{+/-}$ and *Mgll*$^{-/-}$ brain homogenates (n = 4 per genotype) pretreated with either 1 µM JZL184 or DMSO vehicle (30 min at 25 °C) was determined using a previously described liquid chromatography–mass spectrometry assay[27] on an Agilent 6520 QTOF MS.

Brain metabolite measurements. Brain lipid levels were determined as previously described[29] except that free fatty acid levels in *Mgll*$^{+/+}$, *Mgll*$^{+/-}$ and *Mgll*$^{-/-}$ brains were measured on an Agilent 1100 series LC-MS and quantified compared to a palmitic acid calibration curve.

***In situ* hybridization.** Perfused brains from 12-week-old male *Mgll*$^{+/+}$ and *Mgll*$^{-/-}$ mice were postfixed, cryoprotected and frozen as previously described[49]. *In situ* hybridization was performed on 25-µm-thick free-floating coronal sections as described[49] with [^{35}S]UTP-labeled, single-stranded antisense and sense control cRNA probes to *Mgll* cDNA (bases 285–600).

Multidimensional LC-MS proteomic analysis. Mouse brain proteomes (0.75 mg total protein) from *Mgll*$^{+/+}$ and *Mgll*$^{-/-}$ mice (n = 3 mice per genotype) were precipitated with 1:4 chloroform:methanol and denatured with 25 mM ammonium bicarbonate in 6 M urea. Samples were reduced with 10 mM dithiothreitol, alkylated with 40 mM iodoacetamide and diluted to 2 M urea with 25 mM ammonium bicarbonate. Digestion with trypsin (0.5 µg µl^{-1}) was performed overnight at 37 °C in the presence of 1 mM $CaCl_2$. The tryptic peptide samples were acidified with 5% formic acid (wt/vol) and aliquots were frozen at −80 °C until use. Multidimensional protein identification technology (MudPIT) analysis was performed as previously described[27] on an LTQ mass spectrometer (ThermoFinnigan) coupled to an Agilent 1100 series HPLC (n = 2 per genotype, 30 µg protein, 5-step MudPIT) or an LTQ Orbitrap Velos mass spectrometer (ThermoFinnigan) coupled to an Agilent 1200 series HPLC (n = 1 per genotype, 45 µg protein, 10-step MudPIT). The tandem mass spectrometry data were searched against the mouse IPI database using the SEQUEST search algorithm and results were filtered and grouped with DTASELECT. Peptides with cross-correlation scores greater than 1.8 (+1), 2.5 (+2), 3.5 (+3) and delta CN scores greater than 0.08 were included in the spectral counting analysis.

Behavioral assays. To control for stress of repeated injection, all acute treatment groups received 5 d of daily vehicle injections, with acute drug treatment occurring on day 6. Subjects were evaluated 2 h after acute drug administration or the final chronic injection. Acute thermal antinociception was assessed in the tail-immersion test at 56.0 °C using a 10-s cut-off[19]. Surgery for CCI model of the sciatic nerve and allodynia assessment were performed as previously described[18]. Subjects were assessed for mechanical allodynia using von Frey filaments (North Coast Medical) and approximately 30 min later were evaluated for cold allodynia in the acetone-induced paw lifting model, with a maximum cut-off time of 20 s. Cross-tolerance studies in the CCI model were performed starting 26 h following the final chronic drug injection.

Subjects were evaluated for cross-tolerance to WIN55,212-2 or THC 26 or 48 h after the final chronic injection. Cannabimimetic activity was assessed by evaluating mice for catalepsy in the bar test[19], antinociception in the tail immersion test at 52.0 °C[31] and hypothermia by inserting a thermocouple probe 2.0 cm into the rectum. To reduce the number of mice required for this study, we evaluated dose-response relationships using a cumulative dosing regimen in which baseline behavioral endpoints were assessed, injections were given every 40 min and subjects were evaluated for each measure 30 min after each injection, with the entire dose-response assessment being completed in less than 4 h[31].

For precipitated withdrawal, mice were challenged with rimonabant (10 mg per kg) 2 h after the final chronic injection and the incidents of paw fluttering, including any tremors or shaking of the front paws, were recorded for a 1-h observation period[50].

Binding assays. CP-55,940–stimulated [^{35}S]GTPγS binding and [^{3}H]-SR141716A binding in whole brains were conducted as previously described[31]. For CP-55,940–stimulated [^{35}S]GTPγS autoradiographs, coronal sections (20 µm) were cut on a cryostat at −20 °C, thaw-mounted onto gelatin-subbed slides and stored desiccated at −80 °C until use. For assay, slides were brought to 20–25 °C, incubated in assay buffer and 0.5% BSA (wt/vol) containing 0.04 nM [^{35}S]GTPγS in the presence or absence (basal) of maximally effective concentrations of CP55,940 (3 µM) and/or vehicle for 2 h at 25 °C. After final incubation, slides were rinsed twice in 50 mM Tris buffer (pH 7.4) at 4 °C and then rinsed in deionized water. The rinsed slides were dried and exposed to Kodak BioMax MR film with [^{14}C] standards for 24–36 h. Films were digitized at 8-bits per pixel with a Sony XC-77 video camera. Regions of interest were selected using anatomical landmarks and measured using ImageJ (US National Institutes of Health).

Electrophysiology slice preparation and testing. In the chronic experiments, subjects were anaesthetized by isoflurane inhalation and decapitated 24–26 h after the final injection. Hippocampal, cortical and caudate putamen slices (300 µm thick) were cut using a vibrating slicer (Leica) and prepared as described previously[20]. In the acute experiments, the slices were perfused with JZL184 (1 µM) or PF-3845 (10 µM) for 40–80 min.

Whole-cell voltage-clamp recordings were made using patch clamp amplifier (Multiclamp 700B) under infrared differential interference contrast microscopy. Data acquisition and analysis were performed using a digitizer (DigiData 1440A) and analysis software pClamp 10 (Molecular Devices). To record IPSCs, we clamped the neurons at −60 mV and filled the pipettes with an internal solution containing 80 mM cesium methanesulfonate, 60 mM CsCl, 5 mM QX-314, 10 mM HEPES, 0.2 mM EGTA, 2 mM $MgCl_2$, 4 mM MgATP, 0.3 mM Na_2GTP

doi:10.1038/nn.2616

and 10 mM sodium phosphocreatine (pH 7.2 with CsOH). Glutamate receptor antagonists 6-cyano-7-nitroquinoxaline-2,3-dione (CNQX, 20 μM) and D-2-amino-5-phosphonovaleric acid (D-AP5, 25 μM) were present in the artificial cerebrospinal fluid throughout the experiments. Series resistance (15–30 MΩ) was monitored throughout the recordings, and data were discarded if the resistance changed by more than 20%. To record fEPSPs, the pipettes were filled with 1 M NaCl, and picrotoxin (50 μM) was present in the artificial cerebrospinal fluid. To evoke IPSCs or fEPSPs, a bipolar tungsten stimulation electrode was placed in the in the stratum radiatum of the CA1 region of hippocampus, in layer V of cingulate cortex or the caudate putamen. All recordings were performed at 32 ± 1 °C by using an automatic temperature controller.

Data analysis and statistics. All results are expressed as mean ± s.e.m. unless otherwise noted. Results were considered to be significant at $P < 0.05$. All lipid quantification and behavioral endpoints were initially evaluated by ANOVA (treatment or genotype) or repeated-measures ANOVA (cumulative dose responses). Following a significant ANOVA, Dunnett's *post hoc* test was performed for comparisons to treatment or genotypic control. Planned comparisons and specific within-drug treatments are noted in figure captions when used, using a Bonferroni test to correct for multiple comparisons. [^{35}S]GTPγS binding experiments were performed in triplicate and all data points are reported as mean ± s.e.m. of four experiments. Nonspecific binding was first subtracted from all binding data. Stimulated binding was determined as agonist-stimulated binding minus basal binding and values are reported as percentage stimulation above basal. All receptor binding experiments were performed in duplicate and reported as mean ± s.e.m. of four experiments. Nonspecific binding was first subtracted from total binding, yielding specific binding data. Nonlinear regression analyses of agonist concentration effect curves were performed with Prism 5.0 using a sigmoidal dose-response model or specific binding of single site model (GraphPad Software). Values from regressions are reported as mean ± s.e.m. for interpolated results. Regional G protein stimulation autoradiography data are reported as mean ± s.e.m. of triplicate sections from seven to eight brains per group. Net [^{35}S]GTPγS binding is defined as agonist-stimulated [^{35}S]GTPγS binding – basal [^{35}S]GTPγS binding. Analysis was performed in GraphPad Prism Version 5 using Student's *t* test between the two treatments for each individual region analyzed. For electrophysiological analysis, IPSC/f EPSP amplitude was normalized to the baseline. The τ of DSI was measured using a single exponential function of $y = y_0 + k \times e^{-x/\tau}$. The magnitude of DSI was calculated as DSI (%) = 100 × [1 – (mean amplitude of two IPSCs immediately after depolarization divided by mean amplitude of five IPSCs before depolarization)]. Values of 2–3 DSI trials were averaged for each neuron. The depression (%) of IPSCs/fEPSPs by CP55,940 was calculated as 100 × (mean amplitude of IPSCs/fEPSPs during the last 5-min treatment divided by mean amplitude of baseline IPSCs/fEPSPs). Data sets were compared with Student's *t* test.

49. Thomas, E.A. *et al.* Clozapine increases apolipoprotein D expression in rodent brain: towards a mechanism for neuroleptic pharmacotherapy. *J. Neurochem.* **76**, 789–796 (2001).
50. Schlosburg, J.E. *et al.* Inhibitors of endocannabinoid-metabolizing enzymes reduce precipitated withdrawal responses in THC-dependent mice. *AAPS J.* **11**, 342–352 (2009).